Numerical algorithm for simulation of soft tissue swelling and shrinking in a total Lagrangian explicit dynamics framework

Benjamin Zwick, Grand Roman Joldes, Adam Wittek, and Karol Miller

Intelligent Systems for Medicine Laboratory, The University of Western Australia,
35 Stirling Highway, Crawley, WA 6009, Australia.
benjamin.zwick@research.uwa.edu.au
http://school.mech.uwa.edu.au/ISML

Abstract. We present an algorithm for modelling swelling and shrinking of soft tissues based on the total Lagrangian formulation of the finite element (FE) method. Explicit time integration with adaptive dynamic relaxation is used to compute the steady state solution. The algorithm can easily handle geometric and material nonlinearities; and is very efficient because it allows pre-computation of important solution parameters and does not require solution of large systems of equations. Swelling and shrinking behaviour is modelled by applying a multiplicative decomposition of the deformation gradient to separate the total deformation into swelling/shrinking and elastic components. A hyperelastic constitutive law is used to model the elastic behaviour of the material. Accuracy of the algorithm is confirmed by successful verification against an established FE code. The algorithm involves only vector operations and is well suited for parallel implementation for increased computational speed.

Keywords: Finite element method, Biomechanics, Swelling, Growth, Hydrocephalus, Multiplicative decomposition

1 Introduction

Many soft tissue pathologies and their respective treatments are accompanied by swelling or shrinking of the affected area. Examples of swelling include oedema caused by the abnormal accumulation of fluid within the tissue and the mass-effect of tumour growth. Shrinking of tissues can be observed in hydrocephalus and treatments such as osmodiuretics for the reversal of oedema induced swelling.

The biomechanics of swelling and shrinking has been studied in significant detail and models of varying complexity have been suggested. Early studies include lumped parameter models [17] and finite element models with simplified 2D geometry [16]. More recent developments include detailed 3D models based on linear poroelasticity [10], mixture theory [9], models that account for finite deformations [21] and nonlinear material behaviour of the solid phase [1, 2]. Although these models have shown promising results, a significant challenge is presented

by the computational cost involved with solving the complex equilibrium equations that arise from the multiphase mixture theory and the limitations of linear poroelastic models. Within the constrains of the operating theatre results are required quickly and need to be computed on commodity hardware. To enable simulations of entire organs undergoing swelling or shrinking there is a need for computationally efficient and robust solution algorithms.

In this paper, we present an efficient algorithm for modelling swelling and shrinking of soft tissues based on the total Lagrangian (TL) formulation of the finite element (FE) method. In the TL formulation the FE equations are formulated with respect to the initial (undeformed) configuration. Swelling and shrinking behaviour is introduced by applying a multiplicative decomposition of the deformation gradient to separate the total deformation into swelling/shrinking and elastic components. The swelling/shrinking deformation is applied to the initial reference configuration to obtain a (fictitious) intermediate stress-free configuration. The elastic deformation is applied to the intermediate configuration to obtain the final deformed configuration. A hyperelastic constitutive law is used to model the elastic behaviour of the material. We do not consider the physiological cause of the swelling. Instead, we impose a predefined swelling stretch as a predefined function of time. Clearly, this model cannot be used to make predictions of swelling or shrinking but it serves as a demonstration of the method used to enforce swelling and shrinking behaviour in the finite element mesh. Physiological models can be introduced at a later stage to define the amount of swelling/shrinking at each point in the mesh.

The discretised equations are solved using explicit time integration. Adaptive dynamic relaxation [8] ensures rapid convergence towards the steady state solution. A computational advantage of the total Lagrangian over the updated Lagrangian formulations is that all derivatives with respect to the spatial coordinates are calculated with respect to the original configuration and can therefore be pre-computed. The advantage of using explicit time integration with dynamic relaxation for modelling the deformation of soft tissues is that very fast computations are possible compared to similar implicit integration schemes. The stable time step for the explicit method is directly related to the elastic modulus of the material. Compared to structural materials such as steel, soft tissues have a low modulus of elasticity, which allows relatively large time steps to be used making the method especially attractive for modelling soft tissue deformations [15].

2 Methods

2.1 Total Lagrangian formulation of swelling and shrinking

A *motion* or deformation of a continuum body $\mathcal{B} \in \mathbb{R}^3$ is a one-to-one (bijective) mapping [4, 12, 19]

$$\boldsymbol{\varphi}_t : \mathcal{B} \to \mathcal{S}_t \in \mathbb{R}^3, \tag{1}$$

that maps particles $\boldsymbol{X} \in \mathcal{B}$ from the reference configuration $\mathcal{B}$ onto positions

$$\boldsymbol{x} = \boldsymbol{\varphi}_t(\boldsymbol{X}) = \boldsymbol{\varphi}(\boldsymbol{X}, t), \tag{2}$$

in the current configuration $\mathcal{S}_t \subset \mathbb{R}^3$ at time $t \in [0, T]$. A fundamental measure of deformation is the deformation gradient [19]

$$\boldsymbol{F}(\boldsymbol{X}, t) = D\boldsymbol{\varphi}(\boldsymbol{X}) = \partial \boldsymbol{x} / \partial \boldsymbol{X}. \tag{3}$$

To ensure that the deformation between the spatial and material coordinates is invertible and that the local condition of impenetrability of matter is not violated the Jacobian determinant must satisfy [19]

$$J(\boldsymbol{X}) = \det[F(\boldsymbol{X})] > 0. \tag{4}$$

Deformation due to swelling or shrinking can be introduced by considering a (fictitious) stress-free intermediate configuration $\bar{\mathcal{B}}_{st}$ between the initial configuration $\mathcal{B}$ and the deformed configuration $\mathcal{S}_t$ (Fig. 1). This concept was first developed by Flory and Rehner [7] for swelling of polymers [5] and is similar to that used for metal plasticity [19], thermal expansion [11] and biological growth [18]. The total deformation $\boldsymbol{F}$ can be separated into elastic $\boldsymbol{F}^e$ and swelling deformation $\boldsymbol{F}^s$ by a local multiplicative decomposition of the form [2, 11, 18]

$$\boldsymbol{F} = \boldsymbol{F}^e \boldsymbol{F}^s. \tag{5}$$

The deformation caused by swelling ($J^s > 1$) and shrinking ($J^s < 1$) are mathematically equivalent; henceforth the term swelling will be used exclusively to refer to the volume change of the tissue.

It should be understood that $\boldsymbol{F}^e$ and $\boldsymbol{F}^s$ are not proper gradients and that the intermediate configuration is incompatible in a global sense as indicated by the overlapping neighbourhoods $\mathcal{O}_{\boldsymbol{\xi}_1}$ and $\mathcal{O}_{\boldsymbol{\xi}_2}$ of the points $\boldsymbol{\xi}_1, \boldsymbol{\xi}_2 \in \bar{\mathcal{B}}_{st}$ Fig. (1) [13, 19]. Conceptually, the multiplicative decomposition can be thought of as the disassembly of a finite element mesh (the initial undeformed configuration) and the subsequent application of the local volumetric deformation due to swelling on the individual elements. Unless the swelling deformation is homogeneous, this intermediate configuration will be incompatible at the boundaries between elements and the elements will no longer "fit together" (more precisely, the intermediate configuration is not a proper configuration because—except for the special case of homogeneous swelling—a bijective mapping between the material particles and $\mathbb{R}^3$ does not exist [6]). Compatibility of the final (deformed) configuration is enforced by reassembling the mesh using the nodal connectivity of the elements. For a formal exposition of the geometrical details the reader is referred to [6, 12, 13].

For isotropic swelling the swelling deformation gradient can be written as

$$\boldsymbol{F}^s = \lambda_s \boldsymbol{I}, \tag{6}$$

where λ_s is the isotropic swelling stretch and $\boldsymbol{I}$ is the identity tensor. The elastic deformation gradient can then be expressed simply as

$$\boldsymbol{F}^e = \boldsymbol{F} \left(\boldsymbol{F}^s\right)^{-1} = (\lambda_s)^{-1} \boldsymbol{F}. \tag{7}$$

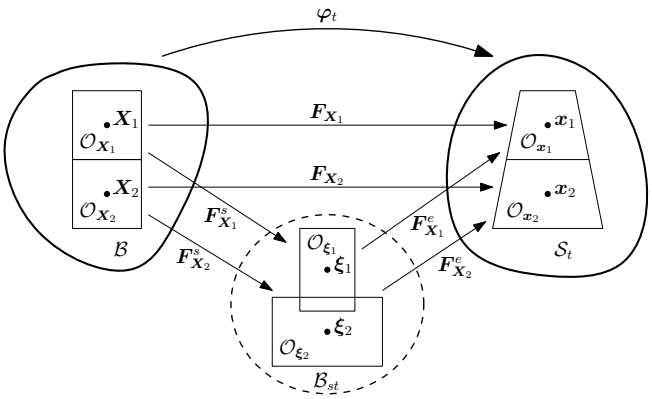

Fig. 1. Multiplicative decomposition of the deformation gradient $\boldsymbol{F} = \boldsymbol{F}^e\boldsymbol{F}^s$ for the motion of two adjacent material points $\boldsymbol{X}_1, \boldsymbol{X}_2 \in \mathcal{B}$ to the spatial positions $\boldsymbol{x}_1, \boldsymbol{x}_2 \in \mathcal{S}_t$.

The total Lagrangian (TL) formulation of the finite element method uses rotation invariant measures of strain (Green–Lagrange strain $\boldsymbol{E}$) and stress (second Piola–Kirchhoff stress $\boldsymbol{S}$) that are calculated with respect to the initial (undeformed) reference configuration $\mathcal{B}$ [3, 4]. The deformations $\boldsymbol{F}^e$ and $\boldsymbol{F}^s$ satisfy the invertibility and impenetrability of matter requirements so that the usual push-forward and pull-back operations can be performed to obtain the stress measures with respect to the configurations $\mathcal{B}$, $\bar{\mathcal{B}}_{st}$ and $\mathcal{S}_t$ [13]. For convenience, the (effective) elastic second Piola–Kirchhoff stress $\boldsymbol{S}^e$ is introduced by the push-forward of $\boldsymbol{S}$ onto the relaxed intermediate configuration $\bar{\mathcal{B}}_{st}$ scaled by the volume ratio J^s. The (total) second Piola–Kirchhoff stress with respect to the initial reference configuration $\mathcal{B}$ can then be expressed as

$$\boldsymbol{S} = J^s(\boldsymbol{F}^s)^{-1}\boldsymbol{S}^e(\boldsymbol{F}^s)^{-T}. \tag{8}$$

In practice, when using hyperelastic materials with the TL formulation of the FE method, $\boldsymbol{S}^e$ is computed using invariants of the elastic deformation gradient $\boldsymbol{F}^e$; whereas, the nodal forces are usually computed using $\boldsymbol{S}$ and the total deformation gradient $\boldsymbol{F}$ with respect to the initial reference configuration [3, 4]. This enables the swelling behaviour to be included entirely within the material constitutive model. Standard element formulations can then be used to calculate the element nodal forces and displacements in the usual manner. The Cauchy stress can be obtained using the inverse Piola transformation

$$\boldsymbol{\sigma} = J^{-1}\boldsymbol{F}\boldsymbol{S}\boldsymbol{F}^T. \tag{9}$$

2.2 Constitutive material model

At low strain rates the mechanical behaviour of soft tissues can be characterised using a hyperelastic constitutive law [22]. Viscoelastic effects are ignored due to

the relatively slow loading speed involved with soft tissue swelling (on the order of a few hours).

Hyperelastic materials are characterised by the existence of a strain energy function $W^e(\boldsymbol{C}^e)$ that relates the deformation to the second Piola–Kirchhoff stress

$$\boldsymbol{S}^e = 2\frac{\partial W^e(\boldsymbol{C}^e)}{\partial \boldsymbol{C}^e}. \tag{10}$$

where $\boldsymbol{C}^e = (\boldsymbol{F}^e)^T\boldsymbol{F}^e$ is the elastic right Cauchy–Green deformation tensor [4]. For hyperelastic materials that are isotropic with respect to the initial, unstressed configuration the strain energy density $W^e(I_1^e, I_2^e, I_3^e)$ can be expressed in terms of the principal invariants $I_1^e = \operatorname{trace}\boldsymbol{C}^e$, $I_2^e = \frac{1}{2}\{(\operatorname{trace}\boldsymbol{C}^e)^2 - \operatorname{trace}(\boldsymbol{C}^e)^2\}$ and $I_3^e = \det\boldsymbol{C}^e$ [4]. The classical (incompressible) neo-Hookean model with strain energy density $W^e(I_1^e) = \mu(I_1^e - 3)$ is based on the assumption that the deformation is isochoric ($J^e = 1$). To account for (slight) compressibility of the material we use the modified strain energy density [23]

$$\bar{W}^e(I_1^e, J^e) = \tfrac{1}{2}\mu\left((J^e)^{-2/3}I_1^e - 3\right) + \tfrac{1}{2}\kappa(J^e - 1)^2, \tag{11}$$

where $J^e = \det\boldsymbol{F}^e$ is used in place of $I_3^e = \det\boldsymbol{C}^e = (J^e)^2$, and μ and κ are the material constants. The behaviour for infinitesimal strains is identical to a linear isotropic elastic model with shear modulus μ and bulk modulus κ. The second Piola–Kirchhoff stress is computed as

$$\boldsymbol{S}^e = \mu(J^e)^{-2/3}\boldsymbol{I} + \left(-1/3\mu(J^e)^{-2/3}I_1^e + \kappa J^e(J^e - 1)\right)(\boldsymbol{C}^e)^{-1}, \tag{12}$$

with respect to the relaxed intermediate configuration $\bar{\mathcal{B}}_{st}$. The strain energy density defined above is equivalent to the neo-Hookean model available in the commercial FE software Abaqus [20] that will be used to verify our algorithm.

2.3 Numerical algorithm for swelling

Our aim is to determine the configuration of the tissue after swelling or shrinking takes place; therefore, we are interested in the steady state solution. Our algorithm is based on the total Lagrangian formulation of the FE method and uses explicit time integration with adaptive dynamic relaxation to compute the steady state solution [3, 4, 8, 15].

1. Initialisation:
   (a) Compute shape function derivative matrices $\boldsymbol{B}_0^m$ at each Gauss point m.
   (b) Compute and diagonalise (constant) mass matrix $\boldsymbol{M}$.
   (c) Initialise nodal displacement $\boldsymbol{d}_0 = \boldsymbol{0}$, $\boldsymbol{d}_1 = \boldsymbol{0}$.
2. Time stepping (n is the step number and Δt is the time step):
   (a) Loop over Gauss points m:
      i. Compute total deformation gradient $\boldsymbol{F}_n^m = \boldsymbol{I} + \boldsymbol{B}_0^m\boldsymbol{d}_n^m$.
      ii. Compute elastic deformation measures $\boldsymbol{F}_n^{e,m}$, $\boldsymbol{C}_n^{e,m}$, $I_{1\,n}^{e,m}$ and $J_n^{e,m}$.
      iii. Compute second Piola–Kirchhoff stress $\boldsymbol{S}_n^m$ using (8).

iv. Compute internal nodal forces $\boldsymbol{f}_n^{\text{int},m} = \boldsymbol{F}_n^m \boldsymbol{S}_n^m \boldsymbol{B}_0^m \bar{w}^m$ where $\bar{w}^m$ are the quadrature weights.
v. Scatter $\boldsymbol{f}_n^{\text{int},m}$ to global force vector $\boldsymbol{f}_n^{\text{int}}$.

(b) Obtain net nodal reaction forces $\boldsymbol{f}_n = \boldsymbol{f}_n^{\text{ext}} - \boldsymbol{f}_n^{\text{int}}$.

(c) Update nodal displacements using the central difference formula

$$\boldsymbol{d}_{n+1} = \boldsymbol{d}_n + \beta\,(\boldsymbol{d}_n - \boldsymbol{d}_{n-1}) + \alpha \boldsymbol{M}^{-1} \boldsymbol{f}_n, \tag{13}$$

where $\alpha = 2\Delta t^2/(2 + c\Delta t)$ and $\beta = (2 - c\Delta t)/(2 + c\Delta t)$. The damping coefficient c is calculated using an adaptive procedure to obtain optimum convergence towards the steady state solution [8].

(d) Check termination criteria [8].

2.4 FE model for algorithm verification

To verify the proposed algorithm we solved a simple model and compared the results to those obtained using a thermal expansion analogy with the commercial FE code Abaqus [20]. We used a cylinder with diameter and height of 10 cm meshed using 35598 linear tetrahedral elements and 6710 nodal points. The nodes on both end surfaces of the cylinder were fully constrained. The swelling stretch was applied using a smooth (3-4-5 polynomial) loading curve [15]

$$\lambda_s(t) = (10 - 15t + 6t^2)t^3, \tag{14}$$

where t is the relative time (varying from 0 to 1). The material parameters of the hyperelastic material model (Sec. 2.2) were chosen to match the behaviour of brain tissue with a mass density of 1000 kg/m^3, Young's modulus in the undeformed state equal to 3000 Pa and Poisson's ratio of 0.49 [14].

Abaqus does not offer swelling behaviour of hyperelastic materials so we used the following thermal expansion analogy. The stretch in each principal direction for an unconstrained material undergoing isotropic thermal expansion is

$$\lambda_\theta = (1 + \alpha\Delta\theta), \tag{15}$$

where α is the thermal expansion coefficient and $\Delta\theta$ is the temperature measured with respect to the reference temperature. By setting $\alpha = 1$ the temperature change is related to the isotropic swelling stretch used in our algorithm by

$$\lambda_s \equiv \lambda_\theta = 1 + \Delta\theta. \tag{16}$$

The steady state solution was obtained using the algorithm described in Sec. 2.3 and compared to the Abaqus/Standard [20] static solution.

3 Results

Simulations of constrained swelling and shrinking were performed to verify the proposed algorithm (Sec. 2.4). The results (Fig. 2) show excellent agreement between the proposed algorithm and the Abaqus/Standard [20] static solution for both the reaction forces and the displacements .

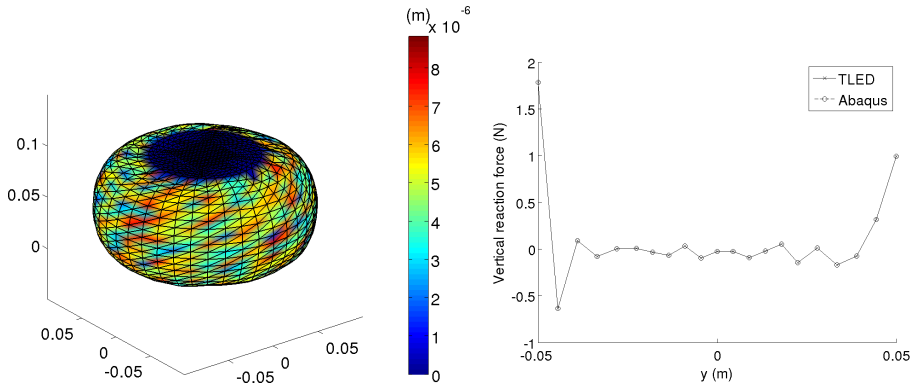

(a) Swelling ($\lambda = 1.5$)

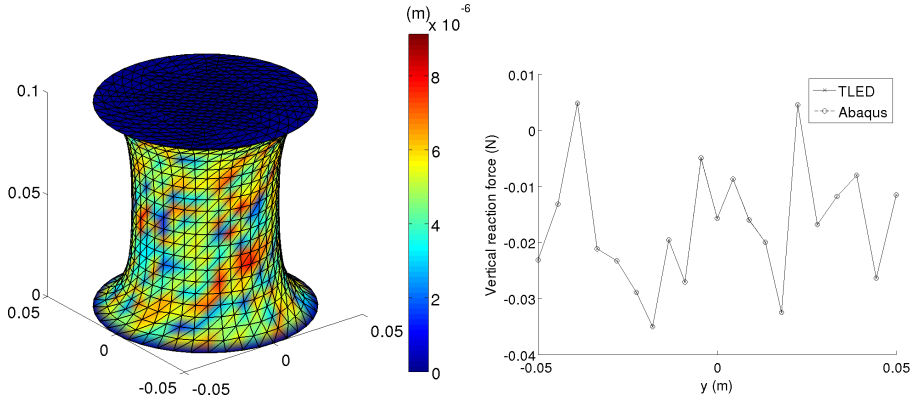

(b) Shrinking ($\lambda = 0.8$)

Fig. 2. Differences in displacements (left) and vertical nodal reaction forces along a line of nodes on the bottom face (right) between our solution method and the equivalent thermal expansion analysis in Abaqus/Standard. The lack of symmetry of the reaction forces is due to the discretisation.

4 Conclusions

We developed an algorithm for modelling swelling and shrinking of soft tissues based on the total Lagrangian formulation of the FE method with explicit time integration and adaptive dynamic relaxation used to compute the steady state solution. The algorithm can easily handle nonlinearities; and is very efficient because it allows pre-computation of important solution parameters and does not require solution of large systems of equations. The algorithm was successfully verified against an established FE code and is well suited for parallel implementation on graphics processing units (GPUs) for increased computational speed.

References

1. Ateshian, G.A., Maas, S., Weiss, J.A.: Multiphasic finite element framework for modeling hydrated mixtures with multiple neutral and charged solutes. Journal of Biomechanical Engineering 135(11), 111001 (11 pages) (2013)
2. Azeloglu, E.U., Albro, M.B., Thimmappa, V.A., Ateshian, G.A., Costa, K.D.: Heterogeneous transmural proteoglycan distribution provides a mechanism for regulating residual stresses in the aorta. American Journal of Physiology - Heart and Circulatory Physiology 294(3), H1197–H1205 (2008)
3. Bathe, K.J.: Finite Element Procedures. Prentice Hall, Englewood Cliffs, N.J (1996)
4. Belytschko, T., Liu, W.K., Moran, B.: Nonlinear Finite Elements for Continua and Structures. John Wiley & Sons, Chichester (2006)
5. Duda, F.P., Souza, A.C., Fried, E.: A theory for species migration in a finitely strained solid with application to polymer network swelling. Journal of the Mechanics and Physics of Solids 58(4), 515–529 (2010)
6. Dvorkin, E.N., Goldschmit, M.B.: Nonlinear continua. Springer (2006)
7. Flory, P.J., Rehner, J.J.: Effect of deformation on the swelling capacity of rubber. The Journal of Chemical Physics 12(10), 412–414 (1944)
8. Joldes, G.R., Wittek, A., Miller, K.: An adaptive dynamic relaxation method for solving nonlinear finite element problems. application to brain shift estimation. International Journal for Numerical Methods in Biomedical Engineering 27(2), 173–185 (2011)
9. Lai, W.M., Hou, J.S., Mow, V.C.: A triphasic theory for the swelling and deformation behaviors of articular cartilage. Journal of Biomechanical Engineering 113(3), 245–258 (1991)
10. Li, X., von Holst, H., Kleiven, S.: Influences of brain tissue poroelastic constants on intracranial pressure (ICP) during constant-rate infusion. Computer Methods in Biomechanics and Biomedical Engineering 16(12), 1330–1343 (2013)
11. Lubarda, V.A.: Constitutive theories based on the multiplicative decomposition of deformation gradient: Thermoelasticity, elastoplasticity, and biomechanics. Applied Mechanics Reviews 57(2), 95–108 (2004)
12. Marsden, J.E., Hughes, T.J.R.: Mathematical foundations of elasticity. Prentice-Hall, Inc., Englewood Cliffs N.J. (1983)
13. Maugin, G.A.: Configurational forces: thermomechanics, physics, mathematics, and numerics. Chapman & Hall/CRC, Boca Raton (2010)
14. Miller, K., Chinzei, K.: Mechanical properties of brain tissue in tension. Journal of biomechanics 35(4), 483–490 (2002)
15. Miller, K., Joldes, G., Lance, D., Wittek, A.: Total Lagrangian explicit dynamics finite element algorithm for computing soft tissue deformation. Communications in Numerical Methods in Engineering 23(2), 121–134 (2007)
16. Nagashima, T., Shirakuni, T., Rapoport, I.: A two-dimensional, finite element analysis of vasogenic brain edema. Neurologia medico-chirurgica 30(1), 1–9 (1990)
17. Rapoport, S.I.: A mathematical model for vasogenic brain edema. Journal of Theoretical Biology 74(3), 439–467 (1978)
18. Rodriguez, E.K., Hoger, A., McCulloch, A.D.: Stress-dependent finite growth in soft elastic tissues. Journal of Biomechanics 27(4), 455–467 (1994)
19. Simo, J.C., Hughes, T.J.R.: Computational Inelasticity. Springer, New York (1998)
20. Simulia: Abaqus 6.10 Documentation. Dassault Systémes, Providence, RI, USA (2010)

21. Taylor, Z., Miller, K.: Reassessment of brain elasticity for analysis of biomechanisms of hydrocephalus. Journal of Biomechanics 37(8), 1263–1269 (2004)
22. Wittek, A., Miller, K., Kikinis, R., Warfield, S.K.: Patient-specific model of brain deformation: Application to medical image registration. Journal of Biomechanics 40(4), 919–929 (2007)
23. Zienkiewicz, O.C., Taylor, R.L., Fox, D.D.: The Finite Element Method for Solid and Structural Mechanics. Elsevier Butterworth-Heinemann, 7th edn. (2013)